Check for updates

CO$_2$ activation by permethylpentalene amido zirconium complexes†

Elizabeth A. Hamilton, Alexander F. R. Kilpatrick, Zoë R. Turner, Duncan A. X. Fraser, Jean-Charles Buffet and Dermot O'Hare *

We report the synthesis and characterisation of new permethyl-pentalene zirconium bis(amido) and permethylpentalene zirconium cyclopentadienyl mono(amido) complexes, and their reactivity with carbon dioxide.

Introduction

The foundations of transition metal amido chemistry were laid in the late 1960s and these compounds are now known to span the largest range of coordination numbers and oxidation states of any in the periodic table.[1] According to the Covalent Bond Classification (CBC) method,[2] the vast majority of terminal amido ligands act as LX ligands and this is indicated by a shorter M–N bond length than the sum of the covalent radii of M and N.[15] Donation of π-electron density from the ligand into partially occupied d-orbitals results in a change of geometry around nitrogen from trigonal pyramidal to planar. In group 4 transition metal(IV) ions, these orbitals are vacant and this allows amido ligands to act as versatile substituents that may impart an extra degree of electronic stabilisation to the electron deficient metal centre. Zirconium forms an extensive range of amido complexes that typically exhibit strong M–N bonds, *ca.* 320–420 kJ mol^{-1} in Zr(NR$_2$)$_4$ species. The mean bond strength decreases in the order Zr–O > Zr–Cl > Zr–N > Zr–C.[3]

The O'Hare group has pioneered the organometallic chemistry of permethylpentalene (η^8-C$_8$Me$_6$ = Pn*), in particular that of the group 4 metals, Ti, Zr and Hf.[4–6] The key entry point for Pn* zirconium chemistry is {Pn*Zr(μ-Cl$_{3/2}$)}$_2$(μ-Cl$_2$)·LiTHF$_x$,[7] a halide-bridged cluster in which the electron deficiency of a theoretical 14 VE "Pn*ZrCl$_2$" species is alleviated through dimerisation and incorporation of LiCl. This results in an 18 VE di-zirconium complex with distorted octahedral coordination geometry about each Zr^{IV} centre.

The reaction of {Pn*Zr(μ-Cl$_{3/2}$)}$_2$(μ-Cl$_2$)·LiTHF$_x$ with LiCp' reagents afforded a series of 18 VE mixed-sandwich complexes, Pn*ZrCp'Cl, which are highly active precatalysts for ethylene polymerisation.[8,9] The 16 VE bis(allyl) complex, Pn*Zr(η^3-C$_3$H$_5$)$_2$, also obtained by salt metathesis, spontaneously reacts with CO$_2$ to give the double-insertion product, Pn*Zr(κ^2-O$_2$CCH$_2$CHCH$_2$)$_2$, which is 18 VE.[10] To extend our investigation of group 4 Pn* chemistry we targeted Zr–N bonds in mono and bis-amido Zr complexes and their subsequent insertion reactions with CO$_2$.

Reactions of transition metal amides with CO$_2$ have been known since 1965,[11] and their carbamic acid derivatives, R$_2$NCO$_2$R', can provide an alternative route to chemicals that are widely used in the pharmaceutical,[12] chemical,[13] and agrochemical industries.[14] This has encouraged significant research into metal complexes for CO$_2$ activation;[15,16] pentalene ligands have shown the ability to stabilise the highly electropositive metal centres typically required, and recent work has established the reactivity of early transition and f-block metal η^8-pentalene metallocenes with CO$_2$ and other small molecules.[17–21]

Carbon dioxide insertion reactions into Zr–N bonds to afford zirconium carbamate complexes are limited to a handful of examples.[22] Homoleptic carbamato complexes, Zr(κ^2-O$_2$CNR$_2$)$_4$, were obtained by exhaustive carbonation of Zr(NR$_2$)$_4$,[23–25] and are active precatalysts for the ring-opening polymerisation of *rac*-lactide.[26] Lappert and co-workers synthesised a heteroleptic complex, Cp$_2$Zr(η^1-OC{O}NMe$_2$)(OAr) (Ar = 2,6-C$_6$H$_3$^{t}Bu$_2$),[27] by carbonation of Cp$_2$Zr(NMe$_2$)(OAr), however, no X-ray structural data were reported to confirm the suggested monodentate binding mode of the carbamate ligand. Chirik and co-workers reported the reaction of CO$_2$ with the dimeric *ansa*-zirconocene dinitrogen complex, [Me$_2$Si(η^5-C$_5$Me$_4$)(η^5-C$_5$H$_3${3-^{t}Bu})Zr]$_2$(μ$_2$-η^2:η^2-N$_2$), which resulted in

Chemistry Research Laboratory, Department of Chemistry, University of Oxford, OX1 3TA Oxford, UK. E-mail: Dermot.ohare@chem.ox.ac.uk

Dalton Transactions

N_2 carboxylation at each nitrogen atom.[28] Erker and co-workers reported reaction of CO_2 with cationic Zr amido complexes, $[Cp_2ZrNRR']^+$ (for R = R' = Ph and R = ^tBu, R' = 3,5-$(C_6H_3(CH_3)_2)$, to afford $[(Cp_2Zr)_2(\mu_2\text{-}\kappa^1O,\kappa^1O\text{-}O_2CNRR')_2]^{2+}$ species, which show bridging coordination of the carbamato moieties.[29]
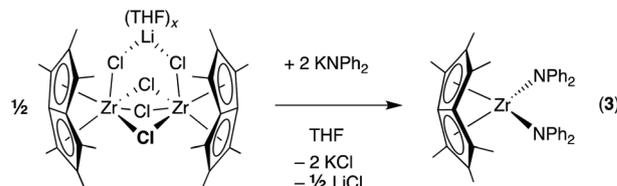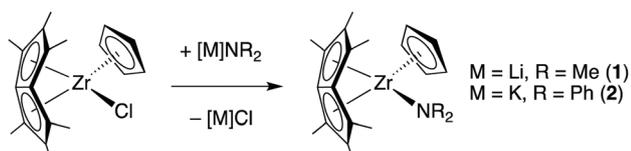
Results and discussion

The reaction of Pn*ZrCpCl,[8] with $LiNMe_2$ in benzene at room temperature over 3 days afforded a yellow solution and cream precipitate of LiCl (Scheme 1). Subsequent workup and recrystallisation from hexane at −80 °C furnished a yellow microcrystalline solid of Pn*ZrCp(NMe$_2$) (**1**) in good yield (83%). Similarly, an ampoule was charged with Pn*ZrCpCl and $KNPh_2$ and pre-cooled THF was added at −78 °C. The reaction was allowed to warm to room temperature and stirred for 16 h, which following workup and recrystallisation from a pentane-toluene mixture at −80 °C, furnished the yellow microcrystalline solid Pn*ZrCp(NPh$_2$) (**2**) in 60% yield (Scheme 1). However, the reaction of **2** in benzene required 1.7 equivalents of $KNPh_2$ for full conversion of Pn*ZrCpCl and this resulted in a 63 : 37 mixture of complex **2** and bis(amido) complex Pn*Zr (NPh$_2$)$_2$ (**3**) (*vide infra*).

The identities and purity of **1** and **2** were confirmed by ^1H and $^{13}C\{^1H\}$ NMR spectroscopy, mass spectrometry, elemental analysis and X-ray crystallography. The ^1H NMR spectra of **1** and **2** show five sharp singlets for the carbocyclic ligands in a 5 : 6 : 6 : 6 integration ratio, which is consistent with C_s molecular symmetry (Fig. S1†). Three singlets between 1.67–2.11 ppm define the Pn*-Me groups, with the wingtip methyl (WT-Me) proton resonance found at a higher chemical shift than the two non-wingtip methyl (NWT-Me) proton resonances. A singlet around 5.50 ppm is assigned in both spectra to protons of the Cp ligand. This lies close to the corresponding resonance in compound Pn*ZrCpCl (5.65 ppm) and at a lower chemical shift to the respective resonance in PnZrCpCl (6.03 ppm).[30] This reflects the increased inductive electron donation resulting from the Pn* methyl groups.

The reaction of $\{Pn^*Zr(\mu\text{-}Cl_{3/2})\}_2(\mu\text{-}Cl_2)\cdot LiTHF_x$ with $KNPh_2$ at room temperature resulted in a yellow solution and cream precipitate of KCl (Scheme 2). Workup and cooling of a hexane solution to −80 °C resulted in the isolation of a yellow microcrystalline solid, Pn*Zr(NPh$_2$)$_2$ (**3**), which was isolated in an 88% yield.

Scheme 2 Synthesis of Pn*Zr bis(amido) complex **3**.

The ^1H NMR spectrum of **3** displays five signals consistent with solution phase C_{2v} symmetry (Fig. S2†), which reflects a higher order of symmetry than that found with **1** and **2**. Singlets at 1.77 and 1.87 ppm define the Pn* NWT-Me and WT-Me proton environments respectively, whilst resonances in the aromatic region correspond to the protons of the phenyl ring.

Single crystals of **1**, **2** and **3** suitable for X-ray diffraction studies were grown through evaporation of saturated C_6D_6 solutions at room temperature (Fig. 1 and S7†). The solid-state
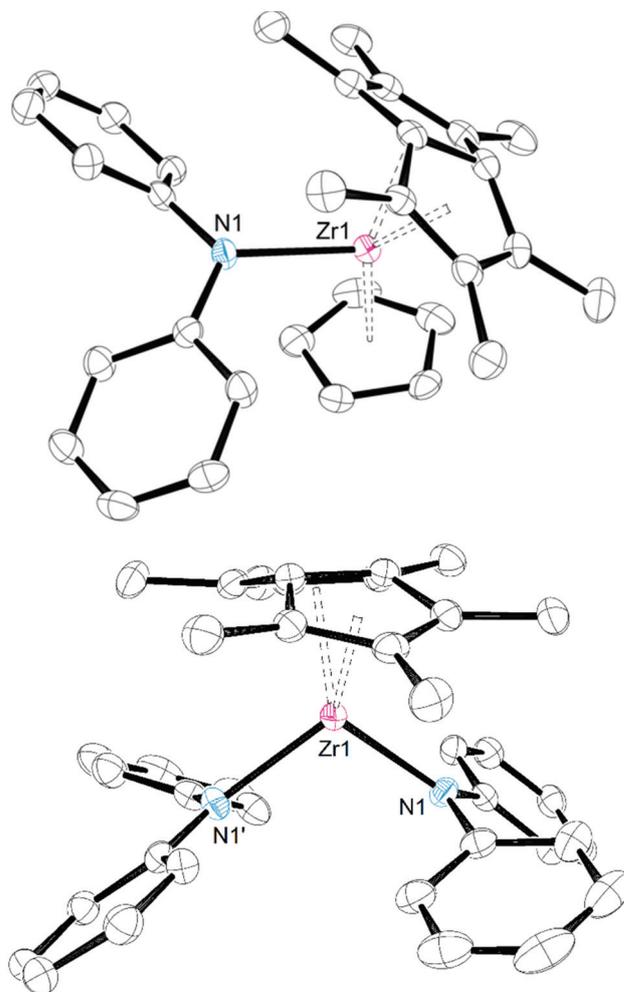
Fig. 1 Solid-state molecular structures of (top) Pn*ZrCp(NPh$_2$) (**2**) and (bottom) Pn*Zr(NPh$_2$)$_2$ (**3**). H atoms are omitted for clarity and thermal ellipsoids are set at 50% probability.

Scheme 1 Synthesis of Pn*Zr Cp mono(amido) complexes **1** and **2**.

structures of **1** and **2** correspond to C_s symmetry, in agreement with the solution phase, with a mirror plane that bisects the molecule through the Pn* bridgehead C–C and Zr–N bonds. By contrast, a descent in symmetry is observed for **3** from C_{2v} in the solution phase to C_2 in the solid state. This results from the loss of the two vertical mirror planes (one that bisects the Pn* WT regions and one that runs along the Pn* bridgehead and Zr–N bonds), which render the NWT-Me resonances equivalent on an NMR timescale. The pentalene fold angles of **1**, **2** and **3** are 30.58°(13), 29.21°(18) and 30.46°(14), respectively (Table 1). These values are similar to pentalene fold angles in {Pn*Zr(μ-Cl$_{3/2}$)}$_2$(μ-Cl$_2$)·LiTHF$_x$ (30.0°) and Pn*ZrCpCl (30.7°),[8] but smaller than those observed in PnZrCpCl (33.0°),[30] which may be attributed to the increased donor capability of the Pn* ligand relative to the unsubstituted pentalene.[31] The angles of N1–Zr–Ct1(Cp)/N1′ in **1**, **2** and **3** are found in a similar range to those of Pn*ZrCpCl (103.3°) and PnZrCpCl (105.2°),[30] which indicates a distortion from idealised tetrahedral geometry (109.5°). C–N–C bond angles around the nitrogen centre are observed to increase from **1** to **2** to **3** (112.5(3)°, 115.5(3)° and 119.0(2)°, respectively) and the sum of the bond angles around each nitrogen correspondingly tend towards to 360° (351.2°, 357.4° and 359.8° respectively). This is attributed to a shift towards sp^2 hybridisation, as the planar arrangement allows for more effective donation of the π-electron density from the N 2p-orbitals to unoccupied Zr 4d-orbitals. For **1** and **2** to be 18 VE complexes the amido ligand would be required to act as a $1e^-$ donor, with corresponding sp^3 hybridisation around the nitrogen atom. By contrast in **3**, it can be rationalised that substitution of a $5e^-$ donating Cp ligand for a second amido ligand requires both nitrogen atoms to act as $3e^-$ donors in order to maintain a 18 VE configuration, which requires sp^2 hybridisation.[32,33] Although changes in hapticity of bound pentalene ligands have been reported, these are extremely rare. One example by Kilpatrick et al. in a titanium bis(oxo) bridged dimer observed a change in hapticity of the pentalene ligand from η^8- to η^5-mode upon addition of pyridine.[17]

Bearing in mind the background outlined in the introduction, the potential of **1**, **2** and **3** to activate CO_2 was investigated. A frozen solution of **1** in C_6D_6 under static vacuum was exposed to an atmosphere of CO_2 (1 bar overpressure) at −78 °C. The reaction mixture was allowed to warm to room temperature and this resulted in an almost instant quantitative conversion of **1** to Pn*ZrCp(η^1-O$_2$CNMe$_2$) (**4**; eqn (S1)†) analogous to the synthesis of M(O$_2$CNMe$_2$)$_4$ (M = Ti, Zr, V).[23,24]

However, by comparison the analogous addition of CO_2 to a frozen solution of **2** in C_6D_6 did not yield a reaction, despite heating at 75 °C for 16 h.

The generally accepted mechanism for d-block metals involves a direct nucleophilic attack of the metal-coordinated nitrogen to carbon dioxide, with the generation of an intermediate N-bound carbamato/carbamic acid moiety.[22] Subsequent rearrangement provides the typical O-coordinated carbamato ligand. The facile reaction of **1** with CO_2 to afford **4**, compared with no reaction observed with **2** and CO_2 can be explained by the lower Lewis basicity of HNPh$_2$ compared with HNMe$_2$. Furthermore, the increased steric congestion around the Zr–N bond in **2** may further retard CO_2 insertion.

Complex **4** was characterised by NMR and IR spectroscopy, elemental analysis and mass spectrometry. The ^1H NMR spectrum revealed singlets at 1.88, 1.98 and 2.09 ppm, which define the Pn*-Me groups (Fig. S3†). These data are in agreement with **4** possessing C_s symmetry in the solution phase, whereby a mirror plane is found bisecting the Pn* bridgehead, Zr–O and Zr–Cp bonds, with the result of one Pn*-Me NWT and two Pn*-WT environments. Singlets at 2.52 ppm and 5.81 ppm were assigned to protons of the NMe$_2$ and Cp ligands respectively. These resonances tend to lie at a higher chemical shifts than the corresponding peaks in the starting material **1** (1.84, 1.90, 2.11, 2.41 and 5.73 ppm respectively), which is attributed to electron withdrawing effect of the carbamate ligand in **4**. The $^{13}C\{^1H\}$ NMR spectrum is consistent with this structure and the characteristic carbamate resonance is located at 166.7 ppm. This demonstrates a contrast between the carbamate and carboxylate moieties the additional contribution of electron density by the nitrogen atom results in a reduced chemical shift with respect to the corresponding peak in carboxylate species Pn*Ti(κ^2-O$_2$CCH$_2$SiMe$_3$)$_2$ (189.8 ppm), Pn*Ti(κ^2-O$_2$CCH$_2^t$Bu)$_2$ (189.9 ppm),[19] and Pn*ZrCp(η^1-O$_2$CC$_3$H$_5$) (188.0 ppm).[10] IR spectroscopy of **4** reveals strong v_a(CO) and v_s(CO) stretches at values at 1564 and 1408 cm^{-1}, respectively. A key determinant in the bonding mode is the difference between these two frequencies compared to the corresponding value of the free carboxylate ion, 164 cm^{-1}.[34,35] The observed difference of 156 cm^{-1} suggests monodentate coordination, in accordance with stretches reported for one of the few reported examples of the Zr(η^1-O$_2$CNMe$_2$) bonding motif in the literature.[27]

The synthesis of Pn*Zr(κ^2-O$_2$CNPh$_2$)$_2$ (**5**) was achieved by the addition of CO_2 (1 bar overpressure) to a frozen solution of **3** at −78 °C. Following work-up and recrystallisation from benzene-d_6, complex **5** was isolated as a white solid in 70% yield (eqn (S2)†). This bidentate CO_2 bonding mode is expected to provide enhanced electronic stability in **5**, relative to the monodentate binding found in **4**.[36] The proposed formulation of **5** is consistent with data from NMR and IR spectroscopy, mass spectrometry, elemental analysis and a single-crystal X-ray diffraction study. The ^1H NMR spectrum of the bis(carbamate) complex **5** shows three resonances in the aliphatic region (1.92, 2.03 and 2.08 ppm), in contrast to the two CH$_3$ resonances observed in the starting material **3** (1.77 and

Table 1 X-ray crystallographic parameters, bond lengths (Å) and angles (°) for complexes **1**, **2** and **3**

	1	**2**	**3**
Zr–N1	2.136(3)	2.236(3)	2.188(2)
Zr–Ct1(Cp)/N1′	2.280(3)	2.2484(17)	2.1191(12)
Zr–Ct2(Pn*)	2.1326(12)	2.1290(14)	2.1191(12)
Zr–Ct3(Pn*)	2.1254(4)	2.1377(18)	2.188(2)
N1–Zr–Ct1(Cp)/N1′	103.77(10)	102.45(9)	107.57(12)
Fold angle	30.58(13)	29.21(18)	30.46(14)

1.87 ppm; Fig. S4†). This reflects a decrease in symmetry on the NMR timescale from the C_{2v} to the C_2 point group. As with **4**, both the aliphatic and aromatic NMR signals of **5** are deshielded with respect to the corresponding signals in the starting complex **3**. The $^{13}C\{^1H\}$ NMR spectrum reflects the reduced symmetry, with three Pn*-Me carbon environments observed compared to the two found in the solution phase of **3**. The bridgehead carbons are found to be equivalent (128.9 ppm), a diagnostic feature for differentiation between C_2 and C_s symmetric Pn* complexes. A singlet carbamate resonance frequency is observed at the highest chemical shift, 167.6 ppm, which is in close agreement with **4**, but slightly below that reported (179.8 ppm) for the similar bidentate complex Pn*Zr$\{\kappa^2$-(O$_2$CCH$_2$CHCH$_2$)$\}_2$. Mesomeric donation is reflected in the IR spectrum of **5**, which shows characteristic bands at 1513 and 1422 cm^{-1} assigned to the $\nu_{as}(CO)$ and $\nu_s(CO)$ carbamate stretches respectively. The separation of these stretching frequencies is significantly less than that observed both in the free ion[35] and **4** and is consistent with bidentate coordination.

A single crystal X-ray diffraction study of **5** confirmed the bidentate coordination mode of the two carbamate ligands (Fig. 2) giving C_2 molecular symmetry, in agreement with the solution phase. Each CO$_2$ molecule inserts to give a four-membered Zr–O–C–O ring, which lies in the same plane as its corresponding nitrogen atom. The sum of the angles around the C and N nitrogen atoms total to exactly 360°, further corroborating the sp^2 hybridisation of the atoms. This heterometallacycle motif is known in other carbamates[37] and suggests added stability from the overlapping π-orbitals. Though no bis (Cp) zirconium complexes with a chelating κ^2-carbamate ligand have been structurally characterised, comparisons can be made between **5** and the heteroleptic and mono(Cp) diethylcarbamate complexes, Zr(κ^2-O$_2$CNEt$_2$)$_4$ and CpZr(κ^2-O$_2$CNEt$_2$)$_3$ (Table S1†).[25] The average Zr–O bond is observed to be marginally longer in **5** (2.239(4) Å) than in Zr(κ^2-O$_2$CNEt$_2$)$_4$

(2.201(2) Å) and CpZr(κ^2-O$_2$CNEt$_2$)$_3$ (2.226(3) Å), attributed to the increased bulk of the Pn* ligand and its enhanced electron donating abilities.

Conclusions

The synthesis and full characterisation of the first mono (amido) Pn*Zr complexes, Pn*ZrCp(NR$_2$) (R = Me, Ph), and the first bis(amido) Pn*Zr complex, Pn*Zr(NPh$_2$)$_2$, have been reported. The amido ligands show interesting versatility in their bonding, acting as both $1e^-$ and $3e^-$ donors to accommodate the electronic requirements of the metal centre. Multiple variants of the amido alkyl substituents have been attempted and it has been observed that whilst small groups encourage dimerisation, larger groups inhibit reactivity. A steric compromise is therefore required to afford the monometallic species.

The zirconium amido species Pn*ZrCp(NR$_2$) {R = Me (**1**), Ph (**2**)} and Pn*Zr(NPh$_2$)$_2$ (**3**) were tested for their reactivity with CO$_2$. This proceeds *via* insertion of the CO$_2$ molecule into the Zr–N bonds resulting in the formation of the carbamate complexes Pn*ZrCp(η^1-O$_2$CNMe$_2$) (**4**) and Pn*Zr(κ^2-O$_2$CNPh$_2$)$_2$ (**5**), respectively. Although both a (Cp)(NR$_2$) and a (NR$_2$)$_2$ ligand set donate $6e^-$ in total, the Cp has a larger steric demand than an amide. Hence, the reactivity of (Cp)(NPh$_2$) is hampered due to the reduced nucleophilicity of the amide (since **1** reacts) and the increased steric protection of the Cp (since **3** reacts) and both factors prevent carboxylation of complex **2**. These results demonstrate the versatility of amido and carbamate as ligands in adapting to the electronic requirements of the metal centre, and further illustrate the ability of Pn* metallocenes to activate small molecules.
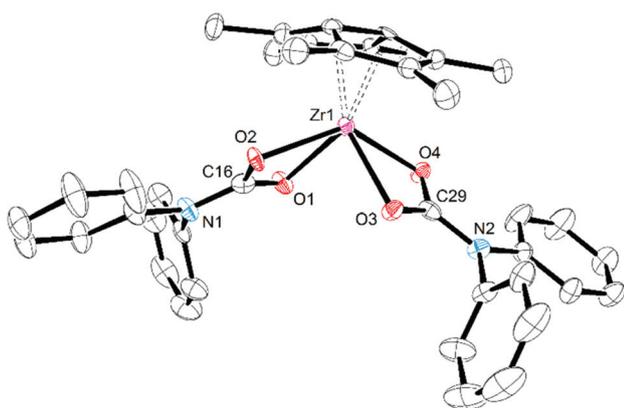
Conflicts of interest

There are no conflicts to declare.

Acknowledgements

Notes and references

1 M. Lappert, A. Protchenko, P. Power and A. Seeber, *Metal amide chemistry*, John Wiley & Sons, 2008.
2 M. Green, *J. Organomet. Chem.*, 1995, **500**, 127–148.
3 M. F. Lappert, D. S. Patil and J. B. Pedley, *J. Chem. Soc., Chem. Commun.*, 1975, 830–831.
4 A. E. Ashley, A. R. Cowley and D. O'Hare, *Chem. Commun.*, 2007, 1512–1514.

Fig. 2 Solid-state molecular structure of Pn*Zr(κ^2-O$_2$CNPh$_2$)$_2$ (**5**). H atoms are omitted for clarity and thermal ellipsoids are set at 50% probability. Selected bond lengths/Å and angles/°: Zr1–O1 2.258(4), Zr1–O2 2.223(4), Zr1–O3 2.250(4), Zr1–O4 2.223(4), N1–C16 1.376(8), N2–C29 1.366(8).

5 F. G. N. Cloke, J. C. Green, A. F. R. Kilpatrick and D. O'Hare, *Coord. Chem. Rev.*, 2017, **344**, 238–262 and references therein.

6 D. D. Clement, S. C. Binding, T. A. Q. Arnold, F. M. Chadwick, I. J. Casely, Z. R. Turner, J.-C. Buffet and D. O'Hare, *Polyhedron*, 2019, **157**, 146–151.

7 R. T. Cooper, F. M. Chadwick, A. E. Ashley and D. O'Hare, *Organometallics*, 2013, **32**, 2228–2233.

8 F. M. Chadwick, R. T. Cooper, A. E. Ashley, J.-C. Buffet and D. O'Hare, *Organometallics*, 2014, **33**, 3775–3785.

9 D. A. X. Fraser, Z. R. Turner, J.-C. Buffet and D. O'Hare, *Organometallics*, 2016, **35**, 2664–2674.

10 F. M. Chadwick, R. T. Cooper and D. O'Hare, *Organometallics*, 2016, **35**, 2092–2100.

11 G. Chandra and M. F. Lappert, *Inorg. Nucl. Chem. Lett.*, 1965, **1**, 83–84.

12 J. Barthelemy, *Lyon Pharm.*, 1986, **37**, 249–263.

13 M. Aresta and E. Quaranta, *Chemtech*, 1997, **27**, 32–40.

14 T. T. Wu, J. Huang, N. D. Arrington and G. M. Dill, *J. Agric. Food Chem.*, 1987, **35**, 817–823.

15 D. B. Dell'Amico, F. Calderazzo, L. Labella, F. Marchetti and G. Pampaloni, *Chem. Rev.*, 2003, **103**, 3857–3898.

16 M. Aresta, A. Dibenedetto and A. Angelini, *Chem. Rev.*, 2014, **114**, 1709–1742.

17 A. F. R. Kilpatrick and F. G. N. Cloke, *Chem. Commun.*, 2014, **50**, 2769–2771.

18 A. F. R. Kilpatrick, J. C. Green and F. G. N. Cloke, *Organometallics*, 2015, **34**, 4816–4829.

19 R. T. Cooper, F. M. Chadwick, A. E. Ashley and D. O'Hare, *Chem. Commun.*, 2015, **51**, 11856–11859.

20 N. Tsoureas, J. Green, F. G. N. Cloke, H. Puschmann, M. Roe and G. J. Tizzard, *Chem. Sci.*, 2018, **9**, 5008–5014.

21 N. Tsoureas, L. Maron, A. F. R. Kilpatrick, R. A. Layfield and F. G. N. Cloke, *J. Am. Chem. Soc.*, 2019, **142**, 89–92.

22 G. Bresciani, L. Biancalana, G. Pampaloni and F. Marchetti, *Molecules*, 2020, **25**, 3603.

23 M. H. Chisholm and M. W. Extine, *J. Am. Chem. Soc.*, 1977, **99**, 792–802.

24 M. H. Chisholm and M. W. Extine, *J. Am. Chem. Soc.*, 1977, **99**, 782–792.

25 F. Calderazzo, U. Englert, C. Maichle-Mössmer, F. Marchetti, G. Pampaloni, D. Petroni, C. Pinzino, J. Strähle and G. Tripepi, *Inorg. Chim. Acta*, 1998, **270**, 177–188.

26 F. Marchetti, G. Pampaloni, C. Pinzino, F. Renili, T. Repo and S. Vuorinen, *Dalton Trans.*, 2013, **42**, 2792–2802.

27 A. W. Duff, R. A. Kamarudin, M. F. Lappert and R. J. Norton, *J. Chem. Soc., Dalton Trans.*, 1986, 489–498.

28 D. J. Knobloch, H. E. Toomey and P. J. Chirik, *J. Am. Chem. Soc.*, 2008, **130**, 4248–4249.

29 A. T. Normand, C. G. Daniliuc, B. Wibbeling, G. Kehr, P. Le Gendre and G. Erker, *J. Am. Chem. Soc.*, 2015, **137**, 10796–10808.

30 K. Jonas, P. Kolb, G. Kollbach and B. Gabor, *Angew. Chem., Int. Ed.*, 1997, **36**, 1714–1718.

31 F. G. N. Cloke, P. B. Hitchcock, M. C. Kuchta and N. A. Morley-Smith, *Polyhedron*, 2004, **23**, 2625–2630.

32 E. Hey-Hawkins, *Chem. Rev.*, 1994, **94**, 1661–1717.

33 D. M. P. Mingos, *J. Organomet. Chem.*, 2004, **689**, 4420–4436.

34 G. Deacon and R. J. Phillips, *Coord. Chem. Rev.*, 1980, **33**, 227–250.

35 K. Ito and H. J. Bernstein, *Can. J. Chem.*, 1956, **34**, 170–178.

36 P. Braunstein and D. Nobel, *Chem. Rev.*, 1989, **89**, 1927–1945.

37 J. A. Higgins Frey, F. G. N. Cloke and S. M. Roe, *Organometallics*, 2015, **34**, 2102–2105.